Chemical Engineering Journal 155 (2009) 627–636

Contents lists available at ScienceDirect

Chemical Engineering Journal

journal homepage: www.elsevier.com/locate/cej

Application of carbon adsorbents prepared from the Brazilian pine-fruit-shell for the removal of Procion Red MX 3B from aqueous solution—Kinetic, equilibrium, and thermodynamic studies

Tatiana Calvete [a], Eder C. Lima [a,*], Natali F. Cardoso [a], Silvio L.P. Dias [a], Flavio A. Pavan [b]

[a] Institute of Chemistry, Federal University of Rio Grande do Sul, UFRGS, Av. Bento Gonçalves 9500, Postal Box 15003, ZIP 91501-970, Porto Alegre, RS, Brazil
[b] Federal University of Pampa, UNIPAMPA, Bagé, RS, Brazil

ARTICLE INFO

Article history:
Received 8 April 2009
Received in revised form 20 August 2009
Accepted 22 August 2009

Keywords:
Adsorption
Brazilian pine-fruit-shell
Activated carbon
Procion Red MX 3B dye
Simulated dyehouse effluent

ABSTRACT

Activated (AC-PW) and non-activated (C-PW) carbonaceous materials were prepared from the Brazilian pine-fruit-shell (*Araucaria angustifolia*) and tested as adsorbents for the removal of Procion Red MX 3B dye (PR-3B) from aqueous effluents. The activation process lead to increase in the specific surface area, average porous volume, and average porous diameter of the adsorbent AC-PW when compared to C-PW. The effects of shaking time, adsorbent dosage and pH on adsorption capacity were studied. PR-3B uptake was favorable at pHs ranging from 2.0 to 3.0 for C-PW and 2.0 to 7.0 for AC-PW. The contact time required to obtain the equilibrium using C-PW and AC-PW as adsorbents was 6 and 4 h at 298 K, respectively. The values of the function error (F_{error}) of fractionary-order kinetic model was at least 15 times lower than the values obtained with pseudo-first-order, pseudo-second order and Elovich kinetic models, indicating that this kinetic model was better fitted to the experimental results. For equilibrium data the F_{error} values of the Sips isotherm model were at least 4.0 lower than the values of Langmuir, Freundlich, and Redlich-Peterson isotherm models using C-PW and AC-PW as adsorbents. The enthalpy and entropy of adsorption of PR-3B were obtained from adsorption experiments ranging from 298 to 323 K. Simulated dyehouse effluents were used to check the applicability of the proposed carbons for effluent treatment.

1. Introduction

Industrial activity is responsible for generating large volumes of effluents containing hazardous species. Color is one of the most important hazardous species found in industrial effluents which needs to be treated, because the presence of dyes in water reduces light penetration, precluding the photosynthesis of aqueous flora [1,2]. Also, dyes can cause allergy, dermatitis, skin irritation and cancer in humans. There are reports that some dyes may cause mutagenicity in humans [3]. Colored waters are aesthetically objectionable for drinking and other purposes. Therefore, industrial effluents containing dyes need to be treated before being released into the environment.

The most efficient procedure for the removal of synthetic dyes from industrial effluents is the adsorption procedure. This process transfers the dye species from the water effluent to a solid phase thereby keeping the effluent volume to a minimum [4–6]. Subsequently, the adsorbent can be regenerated or stored in a dry place without direct contact with the environment [7–9].

Activated carbon is the most employed adsorbent for toxic specie removal from aqueous effluents because of well-developed pore structures and high internal surface area that lead to its excellent adsorption properties [10]. Besides these physical characteristics, the adsorption capacity is also dependent on the source of the organic material employed for the production of the activated carbon [11], as well as the experimental conditions employed in the activation processes [11].

Activated carbon can be prepared by a variety of chemical [12] and physical [13] activation methods and in some cases by a combination of both types of methods [14]. Chemical activation is the process where the carbon precursor material is firstly treated with aqueous solutions of dehydrating agents (*i.e.* H_3PO_4, $ZnCl_2$, H_2SO_4, KOH). Subsequently the carbon material is dried at 373–393 K to eliminate the water. In a subsequent step the chemically treated carbon material is heated between 673 and 1073 K under nitrogen atmosphere [11,12]. Physical activation consists of a thermal treatment of previously carbonized material with suitable oxidizing gases, such as air at temperatures in the 623–823 K range or 1073–1373 K using steam and/or carbon dioxide [11,13].

Although activated carbon is one of the best adsorbents for dye removal from aqueous solutions, the extensive use of high quality activated carbon for dye removal from industrial effluents is very

* Corresponding author. Tel.: +55 51 3308 7175; fax: +55 51 3308 7304.
E-mail addresses: profederlima@gmail.com, eder.lima@ufrgs.br (E.C. Lima).

1385-8947/$ – see front matter © 2009 Elsevier B.V. All rights reserved.
doi:10.1016/j.cej.2009.08.019

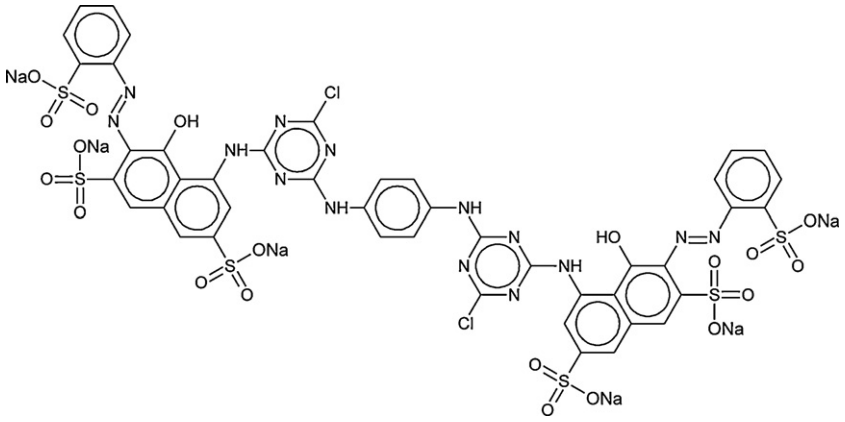

Scheme 1. Structural formulae of Procion Red MX 3B.

expensive, limiting its large application for wastewater treatment [15]. On the other hand, agricultural wastes have low economic value due to their large abundance; additionally, their current deposition creates significant environmental degradation problem. Agricultural waste is a rich source for the activation of carbon production due to its low ash content and reasonable hardness [15]; therefore, conversion of agricultural wastes into activated carbon is a promising alternative to solve environmental problems and also to reduce the costs of activation carbon preparation [15].

There are currently a large number of studies regarding the use of several agricultural wastes to produce activated carbons. Most of them focus on the use of waste materials of considerable rigidity, such as the shells and/or stones of fruits like nuts, peanuts, olives, dates, almonds, apricots and cherries [15]; however, wastes resulting from the production of cereals such as rice, coffee, soybean, maize and corn as well as olive cakes, sugar cane and sugar beat bagasse, coirpith, oil-palm shell (from oil-palm processing mills) and various seed wastes were already used with success [15].

Alternatively to activated carbon, non-activated carbonized materials also present some ability for the removal of dyes from aqueous solutions [16,17] and also presenting the advantage that these materials does not require an activation process at higher temperatures in the presence of special gases.

In the present work, the use of Brazilian pine-fruit-shell (*Araucaria angustifolia* syn. *Araucaria brasiliensis*), is proposed as a precursor for preparation of non-activated carbonaceous materials (C-PW) [17], as well as the activated carbonaceous materials (AC-PW). These adsorbents were successfully used to remove the Procion Red MX 3B dye (PR-3B) from aqueous solutions. The equilibrium, kinetic and thermodynamic data of the adsorption process of the dye onto the adsorbents was investigated.

2. Materials and methods

2.1. Solutions and reagents

De-ionized water was used throughout for solution preparations. Procion Red MX 3B dye (PR-3B) (C.I. 292775; $C_{44}H_{24}Cl_2N_{14}O_{20}S_6Na_6$, 1469.98 g mol^{-1}, see Scheme 1) was obtained from Cotton Química (Novo Hamburgo-RS, Brazil), as a commercially available textile dye, with 70% dye content, and it was used without further purification. The stock solution was prepared by dissolving dye in distilled water to the concentration of 5.00 g L^{-1}. The working solutions were obtained by diluting the dye stock solution to the required concentrations. To adjust the pH solutions, 0.10 mol L^{-1} sodium hydroxide or hydrochloric acid solutions were used. The pH of the solutions was measured using a Hanna (HI 255) pH meter.

2.2. Adsorbents preparation

The Brazilian pine-fruit (piñon) shell was dried and milled as previously reported [18,19]. The carbonization of the Brazilian pine-fruit-shell was achieved as previously reported [17], obtaining the carbonized material assigned as C-PW.

To prepare the activated carbon adsorbent, 10.0 g of previously carbonized material (C-PW) was placed in a quartz reactor provided with a gas inlet and outlet, which was then placed in a vertical cylindrical furnace. In the first step, the sample was heated from room temperature to 1123 K, at a heating rate of 7 K min^{-1} under N_2 atmosphere (flow rate: 100 mL min^{-1}). In step 2, the temperature was kept isothermal for 1.5 h and the gas flow was switched to CO_2 (flow rate: 150 mL min^{-1}). Afterwards, the system was cooled down to room temperature, and the gas was again switched to N_2. The activated carbon obtained was assigned as AC-PW.

2.3. Adsorbent characterization

The N_2 adsorption/desorption isotherms of the adsorbents were obtained at the liquid nitrogen boiling point, in a homemade volumetric apparatus [20], with a vacuum line system employing a turbo molecular Edwards vacuum pump. The pressure measurements were made using a capillary Hg barometer. The apparatus was frequently checked with an alumina (Aldrich) standard reference (150 mesh, 5.8 nm and 155 m^2 g^{-1}). Prior to the measurements, the adsorbent samples were degassed at 250 °C, in vacuum, for 3 h. The specific surface areas were determined from the Brunauer, Emmett and Teller (BET) [21] multipoint method and the pore size distribution were obtained using Barret, Joyner, and Halenda (BJH) method [22].

The points of zero charge (pH_{pzc}) of the adsorbents were determined by adding 20.00 mL of 0.050 mol L^{-1} NaCl to several Erlenmeyer flasks. A range of initial pH (pH_i) values of the NaCl solutions were adjusted from 2.0 to 10.0 by adding either 0.1 mol L^{-1} of HCl and NaOH. The total volume of the solution in each flask was brought to exactly 30.0 mL by further addition of 0.050 mol L^{-1} NaCl solution. The pH_i values of the solutions were then accurately noted and 50.0 mg of C-PW and AC-PW were added to each flask, which were securely capped immediately. The suspensions were shaken in a shaker at 25 °C and allowed to equilibrate for 48 h. The suspensions were then centrifuged at 3600 rpm for 10 min and the final pH (pH_f) values of the supernatant liquid were recorded. The value

Table 1
Kinetic adsorption models.

Kinetic model	Non-linear equation
Avrami	$q_t = q_e\{1 - \exp[-k_{AV}t]^{n_{AV}}\}$
Pseudo-first-order	$q_t = q_e[1 - \exp(-k_f t)]$
Pseudo-second order	$q_t = \frac{k_s q_e^2 t}{1+q_e k_s t}$
	$h_o - k_s q_e^2$ Initial sorption rate
Elovich	$q_t = \frac{1}{\beta}\ln(\alpha\beta) + \frac{1}{\beta}\ln(t)$
Intra-particle diffusion	$q_t = k_{id}\sqrt{t} + C$

of pH_{pzc} is the point where the curve of $\Delta pH\,(pH_f - pH_i)$ *versus* pH_i crosses the line equal to zero [23].

2.4. Adsorption studies

The adsorption studies for evaluation of the C-PW and AC-PW adsorbents for the removal of PR-3B dye from aqueous solutions were carried-out in triplicate using the batch contact adsorption. For these experiments, fixed amount of adsorbents (20.0–200.0 mg) were placed in a 50 mL glass Erlenmeyer flasks containing 20.0 mL of dye solutions (20.00–1500.0 mg L^{-1}), which were agitated for a suitable time (0.25–8 h) at 298–323 K. The pH of the dye solutions ranged from 2.0 to 10.0. Subsequently, in order to separate the adsorbents from the aqueous solutions, the flasks were centrifuged for 10 min. The final concentrations of the dye remaining in the solutions were determined by visible spectrophotometry. Absorbance measurements were made at the maximum wavelength of PR-3B which was 535 nm. The PR-3B detection limit using the spectrophotometric method, determined according to IUPAC [24], was 0.20 mg L^{-1}.

The amount of the dye uptake and percentage of removal of dye by the adsorbents were calculated by applying Eqs. (1) and (2), respectively:

$$q = \frac{(C_o - C_f)V}{m} \quad (1)$$

$$\%\,\text{removal} = \frac{100(C_o - C_f)}{C_o} \quad (2)$$

where q is the amount of dye taken up by the adsorbents (mg g^{-1}), C_o is the initial PR-3B concentration put in contact with the adsorbent (mg L^{-1}), C_f is the dye concentration (mg L^{-1}) after the batch adsorption procedure, V is the volume of dye solution (L) put in contact with the adsorbent and m is the mass (g) of adsorbent.

2.5. Kinetic and equilibrium models

The Avrami, pseudo-first-order, pseudo-second-order, Elovich and the intra-particle diffusion model kinetic equations are given in Table 1 [25].

The Langmuir, the Freundlich, the Sips and the Redlich-Peterson isotherm equations are given in Table 2 [26].

Table 2
Isotherm models.

Isotherm model	Equation
Langmuir	$q_e = \frac{Q_{max}K_L C_e}{1+K_L C_e}$
Freundlich	$q_e = K_F C_e^{1/n_F}$
Sips	$q_e = \frac{Q_{max}K_S C_e^{1/n_S}}{1+K_S C_e^{1/n_S}}$
Redlich-Peterson	$q_e = \frac{K_{RP}C_e}{1+a_{RP}C_e^g}$ where $0 \le g \le 1$

Table 3
Chemical composition of the simulated dyehouse effluents.

Dye	λ (nm)	Concentration (mg L^{-1})	
Reactive dyes			
Procion Red MX 3B	535	100	100
Celmazol Black B	598	20	20
Remazol Brilliant Orange 3B	493	20	20
Reactive Red 194	515	20	20
Direct dyes			
Direct Yellow 4	403	20	20
Direct Blue 53	607	5	5
Auxiliary chemical			
Na_2SO_4		200	200
NaCl		200	200
Na_2CO_3		50	50
CH_3COONa		100	100
CH_3COOH		52,450	800
pH		2.5	5.0

2.6. Statistical evaluation of the kinetic and isotherm parameters

The kinetic and equilibrium models were fitted employing the non-linear fitting method, using the non-linear fitting facilities of the software Microcal Origin® 7.0. In addition, the models were also evaluated by an error function [27], which measures the differences in the amount of dye taken up by the adsorbent predicted by the models and the actual q measured experimentally.

$$F_{error(\%)} = 100x\sqrt{\sum_i^n \left(\frac{q_{i,exp} - q_{i,model}}{q_{i,exp}}\right)^2 \left(\frac{1}{n-p}\right)} \quad (3)$$

where $q_{i,model}$ is the value of q predicted by the fitted model and $q_{i,exp}$ is the value of q measured experimentally, and n is the number of experiments performed, and p is the number of parameter of the fitted model.

2.7. Simulated dyehouse effluent

Two synthetic dyehouse effluents containing four representative reactive dyes plus two direct dyes used for coloring fibers and their corresponding auxiliary chemicals were prepared in two different pH values, using a mixture of different dyes most often applied to textile fibers industries. According to the practical information obtained from a dyehouse, typically 20% of the reactive dyes and 100% of the dyebath auxiliaries remain in the spent dyebath, and its composition suffer a 5–30-fold dilution during subsequent washing and rinsing stages. The concentrations of the dyes and auxiliary chemicals selected to imitate the exhausted dyebath are given in Table 3.

3. Results and discussion

3.1. Characterization of the adsorbents

The physical and chemical properties of C-PW and AC-PW are presented in Table 4. The textural properties of activated carbon prepared from Brazilian pine-fruit-shell (AC-PW) were remarkably changed with the activation process using CO_2. The specific surface area increased more than 2.0-fold, the average pore volume increased by 2.4-fold and the average pore diameter increased by 2.0-fold. These textural parameters suggest that AC-PW could present a better performance compared with C-PW, as adsorbent to remove dyes from aqueous solutions, as reported earlier [1,17].

Table 4
Physical and chemical properties of the adsorbents.

Specific surface area—BET ($m^2\ g^{-1}$)	
C-PW	701
AC-PW	1436
Average pore volume ($cm^3\ g^{-1}$)	
C-PW	0.22
AC-PW	0.56
BJH average pore diameter (nm)	
C-PW	3.95
AC-PW	7.76
Point of zero charge (pH_{pzc})	
C-PW	3.86
AC-PW	7.86

3.2. Effects of acidity on adsorption

One of the most important factors in adsorption studies is the effect of the acidity of the medium [25,26]. Different species will present divergent ranges of suitable pH depending on which adsorbent is used. The effects of initial pH on percentage of removal of PR-3B dye using C-PW and AC-PW were evaluated within the pH range between 2 and 10 (Fig. 1A and B, respectively). For C-PW as adsorbent, the percentage of removal of PR-3B dye was kept practically constant with variations <2.0% in the pH range of 2.0–3.0. When the pH was taken from 3.5 to 10.0 the percentage of dye removal decreased by 36.6%. For AC-PW, the percentage of dye removal was constant for pH solutions ranging from 2.0 up to 7.2. In the pH interval between 8.0 and 10.0, a 19.0% decrease in the percentage of removal was observed. The AC-PW adsorbent shows a larger optimal pH interval for adsorption of PR-3B when compared with C-PW.

The pH_{PZC} for both adsorbents confirm the ranges of optimal pH values for PR-3B removal from aqueous solutions (see Fig. 1). The point of zero charge (pH_{PZC}) for C-PW and AC-PW were 3.86 and 7.86, respectively (see Fig. 1C and D, respectively). For pH values lower than pH_{PZC} the adsorbent presents a positive surface charge [17]. The dissolved PR-3B dye is negatively charged in water solutions. The adsorption of the PR-3B dye takes place when the adsorbent present a positive surface charge. For C-PW, the electrostatic interaction occurs for pH < 3.86, and for AC-PW this interaction occurs for pH < 7.86. The initial pHs of the dye solutions were fixed at 2.5 and 6.0, for C-PW and AC-PW, respectively.

3.3. Adsorbent dosage

The study of adsorbent dosages for the removal of the dye from aqueous solution was carried-out using quantities of C-PW and AC-PW adsorbents ranging from 20.0 to 200.0 mg and fixing the volume and initial dye concentration at 20.0 mL and 100.0 mg L^{-1}, respectively, for both adsorbents. It was observed that highest amount of dye removal was attained for adsorbent masses of at least 50.0 mg of each adsorbent (see Fig. 2A and B). For adsorbent quantities higher than these values, the dye removal remained almost constant. Increases in the percentage of dye removal with adsorbent masses could be attributed to increases in the adsorbent surface areas, augmenting the number of adsorption sites available for adsorption, as already reported in several papers [25,27]. On the other hand, the increase in the adsorbent mass promotes a remarkable decrease in the amount of dye uptake per gram of adsorbent (q), as shown in Fig. 2, an effect that can be mathematically explained by combining Eqs. (1) and (2):

$$q = \frac{\%\text{removal}\ C_o V}{100m} \tag{4}$$

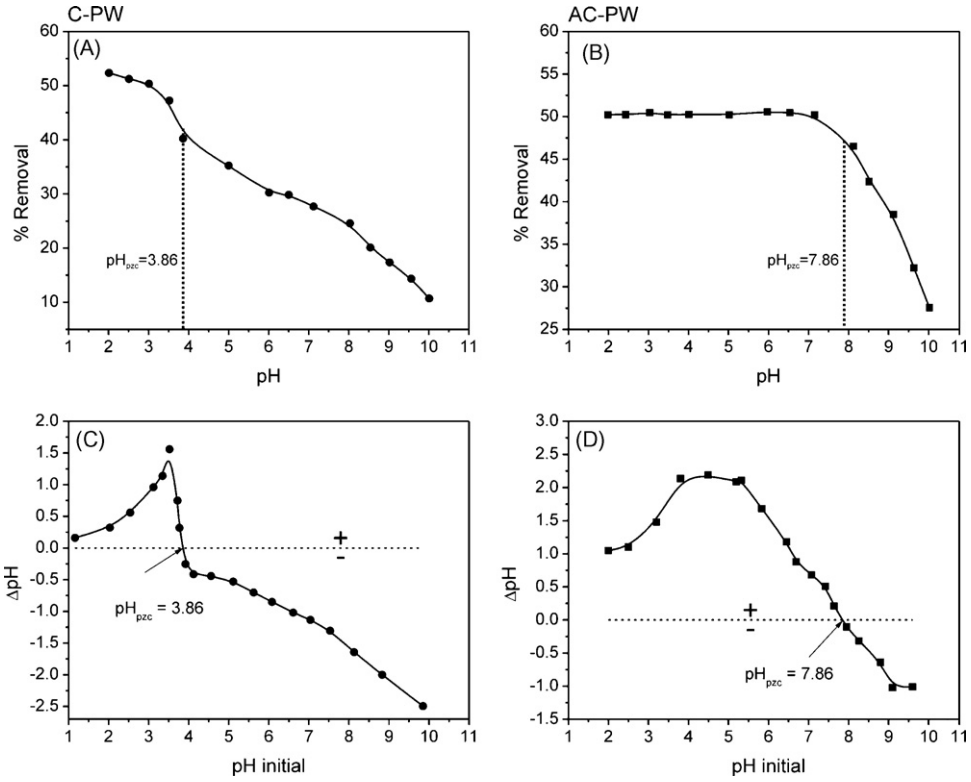

Fig. 1. Effect of pH on the removal of PR-3B from aqueous solution. C-PW (A); AC-PW (B). Points of zero charge for C-PW (C) and AC-PW (D). The initial PR-3B concentrations and adsorbent masses were fixed at 100.0 mg L^{-1} and 30.0 mg for both adsorbents. The contact time between adsorbent and adsorbate was fixed at 4.0 h. The symbols + and − means positive and negative surface charges at the adsorbent surface.

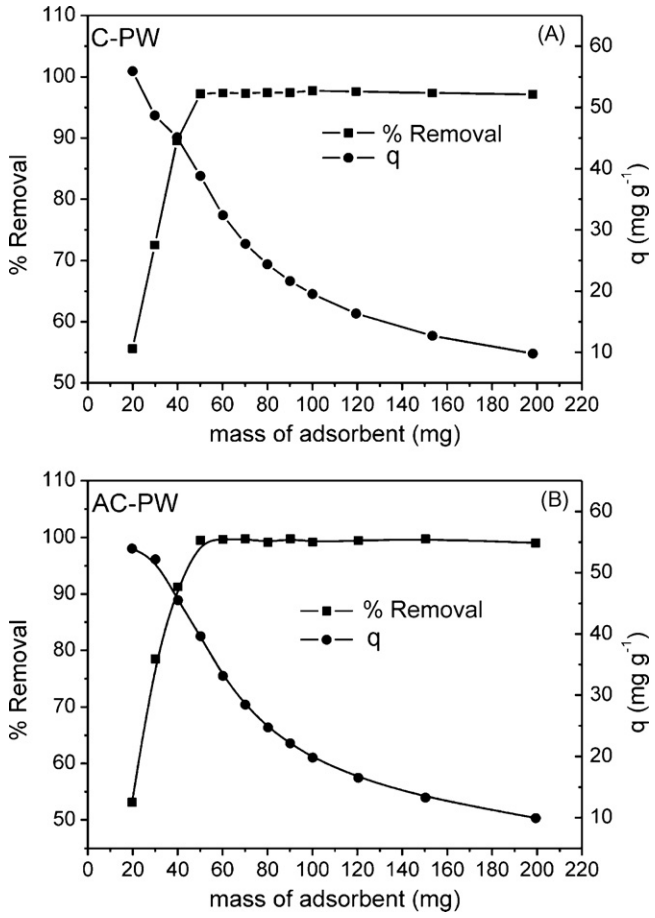

Fig. 2. Adsorbent dosage. C-PW (A) and AC-PW (B).

As observed from Eq. (4), the amount of dye uptake (q) and the mass of adsorbent (m) are inversely proportional. For a fixed dye percentage removal, the increase of adsorbent mass leads to a decrease in q values, since the volume (V) and initial dye concentrations (C_o) are always fixed. These values clearly indicate that the adsorbent mass must be fixed at 50.0 mg, the mass that corresponds to the minimum amount of adsorbent that leads to constant dye removal. The adsorbent masses were therefore fixed at 50.0 mg for both C-PW and AC-PW adsorbents, the minimum amount of adsorbent which leads to a constant removal of PR-3B dye.

3.4. Kinetic studies

Adsorption kinetic studies are important in treatment of aqueous effluents because they provide valuable information on the mechanism of the adsorption process [27].

To study the mechanism of dye adsorption, the kinetic data was fitted using the four kinetic models depicted in Table 1 (Fig. 3A–D).

As can be seen, only the Avrami fractionary kinetic model presented the best fit, presenting low error function values and also high R^2 values, for the two initial concentration levels of the dye with both adsorbents. For clarity, only the Avrami fractionary kinetic order is depicted in Table 5. All other kinetic models are not shown in this table because they presented F_{error} values at least 15 times higher than the Avrami fractionary kinetic model. The lower the error function is, the lower will be the difference of the q calculated by the model from the experimentally measured q [26,27]. Additionally, it was verified that the q_e values found in the fractionary-order were closer to the experimental q_e values, when compared with all other kinetic models. These results indicate that the fractionary-order kinetic model should explain the adsorption process of PR-3B taken up by the C-PW and AC-PW adsorbents.

The Avrami kinetic equation has been successfully employed to explain several kinetic processes of different adsorbents and adsorbates [1,9,17,25,27–33]. The Avrami exponent (n_{AV}) is a fractionary number related with the possible changes of adsorption mechanism that take place during the adsorption process [1,9,17,25,27–33]. Instead of the mechanism of adsorption follows only an integer-kinetic order, the adsorption could follow multiple kinetic orders that are changed during the contact of the adsorbate with the adsorbent [27–33]. The n_{AV} is a resultant of the multiple kinetic order of the adsorption procedure.

Because the kinetic results fitted very well to the fractionary kinetic model (Avrami model) for the PR-3B dye using C-PW and AC-PW adsorbents (see Table 5 and Fig. 3), the intra-particle diffusion model [26] was used to verify the influence of mass transfer resistance on the binding of PR-3B to both adsorbents (see Table 5 and Fig. 3E–H). The intra-particle diffusion constant, k_{id} (mg g^{-1} h$^{-0.5}$, see Table 1), can be obtained from the slope of the plot of q_t (uptake at any time, mg g^{-1}) *versus* the square root of time. Fig. 3E–H shows the plots of q_t *versus* $t^{1/2}$, with multi-linearity for the PR-3B dye using C-PW and AC-PW adsorbents. These results imply that the adsorption processes involve more than one single kinetic stage (or adsorption rate) [27]. For instance, the adsorption process exhibits two stages, which can be attributed to two linear parts (see Fig. 3E–H). The first linear part can be attributed to intra-particle diffusion, which causes a delay in the process [27]. The second stage is the diffusion through smaller pores, which is followed by the establishment of equilibrium [27].

It was observed in Fig. 3A–D, that the minimum contact time of the PR-3B with the adsorbents to reach the equilibration was about 6.0 and 4.0 h, using C-PW and AC-PW as adsorbents, respectively (see Fig. 3A–D). The longer required contact time to reach the equilibrium for C-PW, in comparison with AC-PW, could be attributed to the textural characteristics of the non-activated carbon such as lower average pore volume and average pore diameter (see Table 4) as already reported in the literature [1,17]. The diagonal lengths of PR-3B dye are 2.11 and 2.09 nm, respectively (see Fig. 4); while the BJH average pore diameters of the adsorbents are 3.95 and 7.76 nm for C-PW and AC-PW, respectively. The ratios of average pore diameter of the adsorbents to the maximum diagonal length of PR-3B dye are 1.87 and 3.68, for C-PW and AC-PW, respectively. Therefore the diffusion of PR-3B dye from the bulk adsorbate solution to the pores of C-PW adsorbent may have been limited, thereby delaying the adsorption process. The average pore diameter of the C-PW adsorbent could accommodate only one PR-3B molecule which was diffused from the bulk of adsorbate solution to the pores of the adsorbent. When the AC-PW adsorbent was used, up to three PR-3B molecules could be accommodated by each adsorbent pore. This interpretation is also corroborated by the intra-particle diffusion constant (k_{id}) reported in Table 5, where the obtained values of k_{id} for AC-PW were at least 52.7% higher than those obtained with C-PW [17].

3.5. Equilibrium studies

An adsorption isotherm describes the relationship between the amount of adsorbate taken up by the adsorbent and the adsorbate concentration remaining in solution. There are many equations for analyzing experimental adsorption equilibrium data. The equation parameters of these equilibrium models often provide some insight into the adsorption mechanism, the surface properties and affinity of the adsorbent [26]. In this work, the Langmuir, the Freundlich, the Sips and the Redlich-Peterson isotherm models were tested (see Fig. 5).

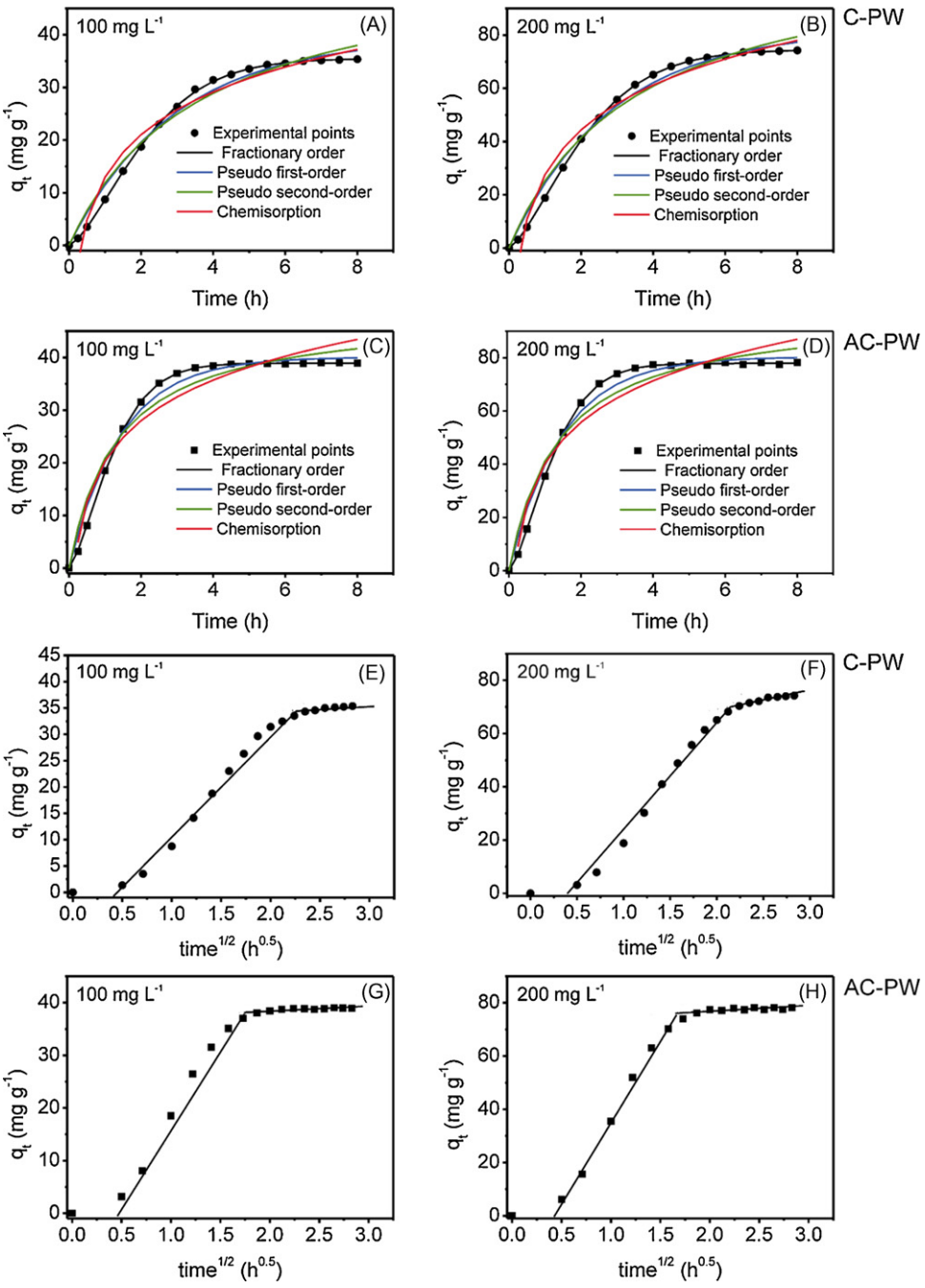

Fig. 3. Kinetic models for the adsorption of PR-3B. (■) C-PW; (●) AC-PW. (A) C-PW 100 mg L^{-1}; (B) C-PW 200 mg L^{-1}; (C) AC-PW 100 mg L^{-1}; (D) AC-PW 200 mg L^{-1}; (E) C-PW 100 mg L^{-1}; (F) C-PW 200 mg L^{-1}; (G) AC-PW 100 mg L^{-1}; (H) AC-PW 200 mg L^{-1}.

The isotherms of adsorption carried-out from 298 to 323 K, of PR-3B on the two adsorbents were performed, using the best experimental conditions described previously (see Table 6). Considering that for a good fitting of a non-linear model, the F_{error} values should be ≤3.0% [25–27]. Based on this confident limit value for $F_{error,}$ for C-PW adsorbent, the isotherm parameters obtained for Langmuir (298–313 K), Freundlich (298–323 K), Redlich-Peterson (298–313 K) have no physical meaning, because the amount adsorbed (q) fitted by the models present an average difference higher than 3.0% of the actual q measured. For AC-PW adsorbent, the isotherm parameters of Langmuir (303–323 K) and Freundlich (298–318 K) are not confident. Based on the F_{error} values analysis the only isotherm model that was well fitted for all temperatures (298–323 K) and both adsorbent was the Sips isotherm model. It should also be stressed that the Redlich-Peterson isotherm model was well fitted for all temperatures using AC-PW adsorbent.

The maximum amounts of PR-3B uptake were 197 and 328 mg g^{-1} (based on the Sips model) for C-PW and AC-PW, respectively, at 323 K. These values indicate that these adsorbents are good adsorbents for PR-3B removal from aqueous solutions.

3.6. Thermodynamic studies

Thermodynamic parameters related to the adsorption process, *i.e.*, Gibb's free energy change (ΔG°, kJ mol^{-1}), enthalpy change (ΔH°, kJ mol^{-1}), and entropy change (ΔS°, J mol^{-1} K^{-1}) are deter-

Table 5
Kinetic parameters for PR-3B removal using C-PW and AC-PW as adsorbents. Conditions: temperature was fixed at 298 K; pH 2.5 for C-PW and pH 6.0 for AC-PW; adsorbent mass 50.0 mg.

	C-PW		AC-PW	
	100 mg L^{-1}	200 mg L^{-1}	100 mg L^{-1}	200 mg L^{-1}
Fractionary-order				
k_{AV} (h^{-1})	0.416	0.421	0.727	0.712
q_e (mg g^{-1})	35.5	74.5	38.9	77.9
n_{AV}	1.46	1.41	1.42	1.45
R^2	0.9998	0.9999	0.9999	0.9999
F_{error} (%)	1.73	0.914	1.45	0.448
Intra-particle diffusion				
$k_{i,1}$ (mg g^{-1} $h^{-0.5}$)[a]	20.3	39.1	31.0	62.3

[a] First stage.

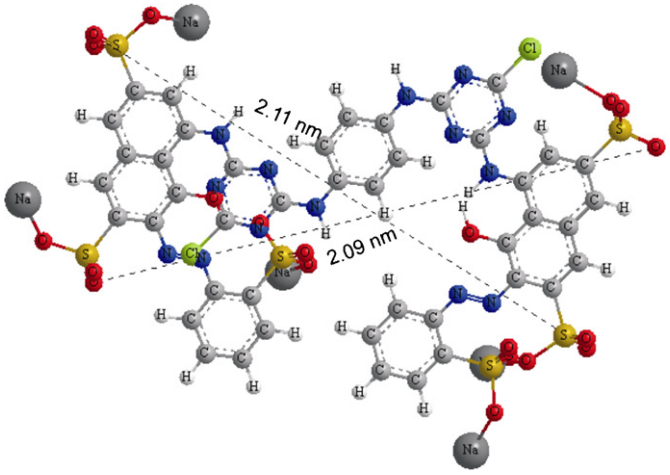

Fig. 4. Optimized three-dimensional structural formulae of PR-3B. The dimensions of the chemical molecule were calculated using ChemBio 3D® version 11.0.1.

mined by the following equations:

$$\Delta G^\circ = \Delta H^\circ - T\,\Delta S^\circ \quad (5)$$

$$\Delta G^\circ = -RT\ln(K) \quad (6)$$

The combination of Eqs. (5) and (6), gives:

$$\ln(K) = \frac{\Delta S^\circ}{R} - \frac{\Delta H^\circ}{R} x \frac{1}{T} \quad (7)$$

where R is the universal gas constant (8.314 J K^{-1} mol^{-1}), T is the absolute temperature (Kelvin) and K represents that adsorption constants of the isotherm fits (K_S—Sips equilibrium constant, which must be converted to SI units, by using the molecular mass of the dye) obtained from the isotherm plots. The ΔH° and ΔS° values can be calculated from the slope and intercept of the linear plot of ln(K) *versus* 1/T.

The thermodynamic results are depicted in Table 7. Taking into account that the Langmuir isotherm parameters were not confident at 3% level for temperature range (298–323 K) using both the adsorbents (C-PW and AC-PW), the thermodynamic parameters were only obtained using the values of Sips equilibrium constant (K_S). The R^2 values of the linear fit were at least 0.99, indicating that the values of enthalpy and entropy calculated for both adsorbents are fairly confident.

The magnitude of enthalpy is consistent with a physical interaction of an adsorbent with an adsorbate as already reported in the literature [34,35]. The enthalpy changes (ΔH°) indicate that adsorption followed endothermic processes. Negative values of ΔG indicated that the PR-3B reactive dye adsorption by C-PW and AC-PW adsorbents were spontaneous and favorable processes for all studied temperatures. The positive values of ΔS° confirm a high preference of PR-3B molecules for the carbon surface of C-PW and AC-PW and also suggest the possibility of some structural changes or readjustments in the dye–carbon adsorption complex [35], and also is consistent with the dehydration of dye molecule before its adsorption to carbon surface, and the releases of these water molecules to the bulk solution.

The increase in adsorption capacities of C-PW and AC-PW at higher temperatures may be attributed to the enhanced mobility and penetration of dye molecules within the adsorbent porous

Table 6
Isotherm parameters for PR-3B adsorption, using C-PW and AC-PW as adsorbents. Conditions: adsorbent mass of 50.0 mg; pH fixed at 2.5 and 6.0 for C-PW and AC-PW, respectively; and using a contact time of 6 and 4 h for C-PW and AC-PW, respectively.

	C-PW						AC-PW					
	298 K	303 K	308 K	313 K	318 K	323 K	298 K	303 K	308 K	313 K	318 K	323 K
Langmuir												
Q_{max} (mg g^{-1})	195	196	196	197	198	198	268	275	267	265	244	240
K_L (L g^{-1})	0.0937	0.0878	0.0861	0.0808	0.0758	0.0741	0.138	0.147	0.161	0.180	0.210	0.229
R^2	0.9858	0.9917	0.9953	0.9982	0.9996	1.000	0.9956	0.9921	0.9826	0.9759	0.9581	0.9294
F_{error} (%)	31.1	8.25	4.91	4.91	1.86	0.249	2.96	4.85	3.27	3.74	4.67	4.29
Freudlich												
K_F (mg g^{-1}(mg L^{-1})$^{-1/n_F}$)	43.4	41.8	43.1	41.8	40.0	39.3	75.0	81.5	86.4	90.5	90.3	97.7
n_F	3.15	3.13	3.19	3.12	3.03	3.01	3.57	3.72	3.90	4.16	4.51	5.00
R^2	0.8496	0.8937	0.9074	0.9212	0.9340	0.9430	0.9521	0.9498	0.9564	0.9660	0.9810	0.9798
F_{error} (%)	97.3	23.5	16.65	25.7	19.2	19.4	7.53	8.83	4.77	4.25	3.14	2.33
Sips												
Q_{max} (mg g^{-1})	176	180	183	188	193	197	292	306	312	317	323	328
K_S ((g L^{-1})$^{-1/n_S}$)	0.0417	0.0477	0.0528	0.0595	0.0671	0.0735	0.173	0.195	0.221	0.251	0.283	0.318
n_S	0.695	0.744	0.790	0.861	0.937	0.995	1.25	1.33	1.46	1.59	1.93	2.15
R^2	1.000	1.000	1.000	1.000	0.9999	1.000	1.000	1.000	1.000	1.000	1.000	1.000
F_{error} (%)	0.751	0.331	0.284	0.367	0.343	0.225	0.159	0.119	0.125	0.145	0.119	0.0953
Redlich-Peterson												
K_{RP} (L g^{-1})	18.3	17.2	16.9	15.9	15.0	14.7	48.7	60.3	78.1	98.8	138	188
a_{RP} (mg L^{-1})$^{-g}$	0.0937	0.0878	0.0861	0.0808	0.0758	0.0741	0.261	0.341	0.503	0.674	1.10	1.50
g	1.00	1.00	1.00	1.00	1.00	1.00	0.919	0.902	0.876	0.867	0.850	0.855
R^2	0.9859	0.9917	0.9953	0.9982	0.9996	1.000	0.9994	0.9990	0.9987	0.9985	0.9987	0.9989
F_{error} (%)	32.5	8.62	5.12	5.13	1.94	0.235	0.639	0.883	1.07	1.20	1.07	0.915

Table 7
Thermodynamic parameters of the adsorption of PR-3B on C-PW and AC-PW adsorbents. Conditions: adsorbent mass of 50.0 mg; pH fixed at 2.5 and 6.0 for C-PW and AC-PW, respectively; and using a contact time of 6 and 4 h for C-PW and AC-PW, respectively.

Sips	Temperature (K)					
	298	303	308	313	318	323
C-PW						
K_S $((\text{mol L}^{-1})^{-1/n_S})$	6.13×10^4	7.00×10^4	7.76×10^4	8.75×10^4	9.87×10^4	1.08×10^5
ΔG (kJ mol^{-1})	−27.3	−28.1	−28.8	−29.6	−30.4	−31.1
ΔH° (kJ mol^{-1})	18.2	–	–	–	–	–
ΔS° (J K^{-1} mol^{-1})	153	–	–	–	–	–
R^2	0.9988	–	–	–	–	–
AC-PW						
K_S $((\text{mol L}^{-1})^{-1/n_S})$	2.54×10^5	2.86×10^5	3.25×10^5	3.69×10^5	4.16×10^5	4.67×10^5
ΔG (kJ mol^{-1})	−30.8	−31.6	−32.5	−33.4	−34.2	−35.1
ΔH° (kJ mol^{-1})	19.6	–	–	–	–	–
ΔS° (J K^{-1} mol^{-1})	169	–	–	–	–	–
R^2	0.9996	–	–	–	–	–

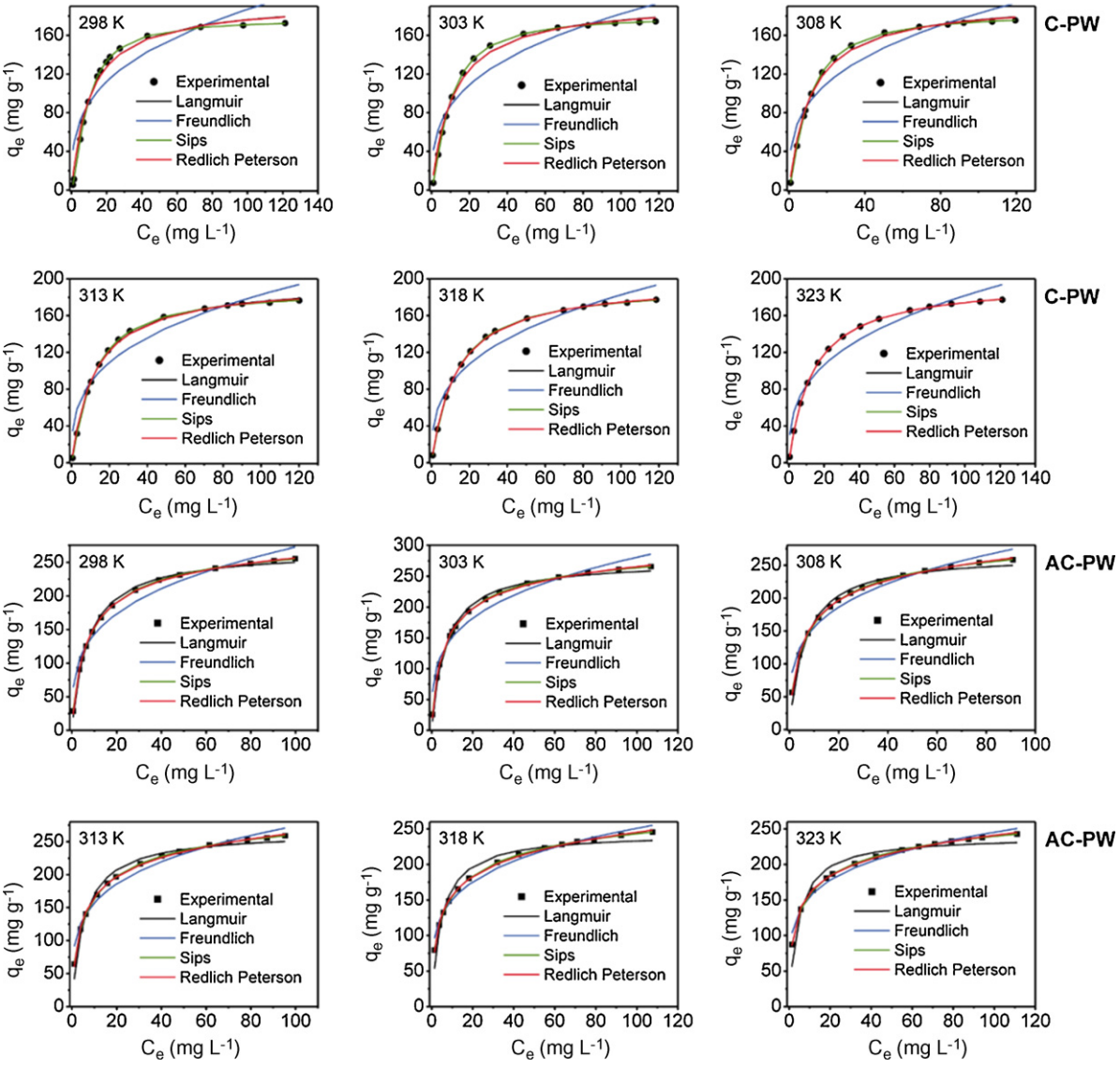

Fig. 5. The equilibrium isotherm for PR-3B adsorption on C-PW and AC-PW adsorbents, using batch contact adsorption procedure. Conditions adsorbent mass of 50.0 mg; pH fixed at 2.5 and 6.0 for C-PW and AC-PW, respectively; and using a contact time of 6 and 5 h for C-PW and AC-PW, respectively.

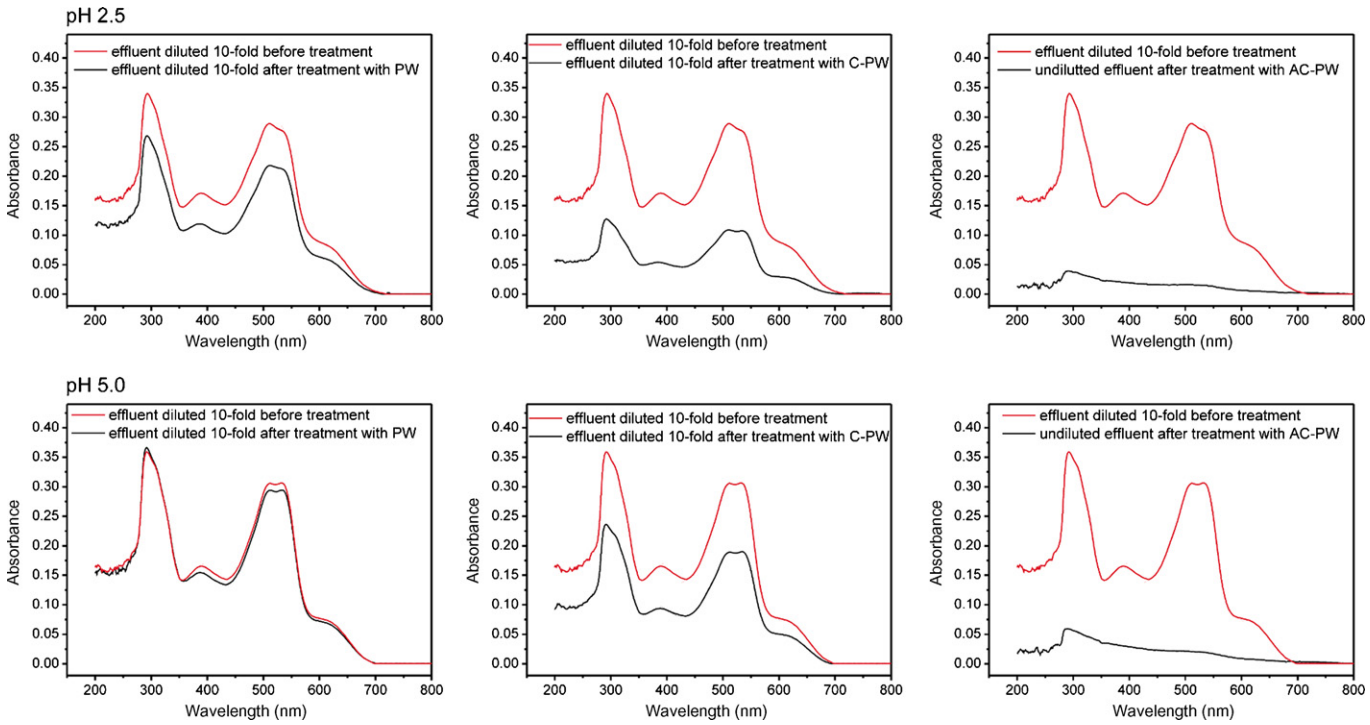

Fig. 6. UV–vis spectra of simulated dye effluents before and after adsorption treatments.

structures by overcoming the activation energy barrier and enhancing the rate of intra-particle diffusion [34,35].

3.7. Treatment of a simulated dyehouse effluent

In order to verify the efficiency of the Brazilian pine-fruit-shell in natural (PW), carbonized form (C-PW) and activated carbon (AC-PW) as adsorbents for the removal of dyes from textile effluents, simulated dyehouse effluents were prepared (see Table 3). The UV–vis spectra of the untreated effluents (pH 2.5 and 5.0) and treated with PW, C-PW and AC-PW were recorded from 200 to 800 nm (Fig. 6). The absorption bands at 293, 389, 511, 535 and 623 nm were utilized to monitor the percentage of dyes mixture removed from the simulated dye effluents. The PW adsorbent removed 26.1% of the dye mixture at pH 2.0 and only 3.9% at pH 5.0. The untreated Brazilian pine-fruit-shell (PW), included in this part of the work, shows the lowest sorption capacity and performance for the removal of dyes from industrial effluents (see Fig. 6A and D) when compared with the two other adsorbents. Its low sorption capacity could be related with this fibrous and compact structure with low specific surface area and low average pore volume and pore diameter, as reported earlier [1]. The C-PW material presents an intermediate performance for the treatment of simulated dye effluents. At pH 2.5, C-PW removed 64.7% of the dye mixture (Fig. 6B), but its value was decreased to 37.7% for dye effluent at pH 5.0. These removal data are consistent with the pH effects on the sorption capacity, and also with the pH_{PZC} describe above for C-PW. On the other hand, AC-PW material was efficient for the treatment of simulated dye effluents at pH values of 2.5 (99.2% removal) as well as 5.0 (98.8% removal). Taking into account that in real applications the pH of effluent for being released to the environment should be close to the natural waters (pH 5.0–6.0), the AC-PW adsorbent is a very good adsorbent for treatment of industrial effluents contaminated with dyes.

The better characteristics of AC-PW such as, higher value of pH_{PZC}, higher specific surface area, higher average pore volume, higher average pore diameter (see Table 4) when compared to C-PW are responsible for its better performance for treatment of dye effluents.

4. Conclusion

The carbonized Brazilian pine-fruit-shell (C-PW) and the activated carbon prepared from Brazilian pine-fruit-shell (AC-PW) are good alternative adsorbents to remove Procion Red MX 3B (PR-3B) from aqueous solutions. Both adsorbents interact with the dye at the solid/liquid interface when suspended in water. The best conditions were established with respect to pH and contact time to saturate the available sites located on the adsorbent surface. Five kinetic models were used to adjust the adsorption and the better fit was the Avrami (fractionary-order) kinetic model, however, the intra-particle diffusion model gave two linear regions, which suggested that the adsorption could be also followed by multiple adsorption rates. The maximum adsorption capacities were 197 and 328 mg g^{-1} for C-PW and AC-PW, respectively. The increased adsorption capacity of AC-PW could be the related to the improvements on the textural characteristics (specific surface area, average pore volume, average pore diameter) of the material after the activation process with CO_2.

The thermodynamic parameters of adsorption (ΔH°; ΔS° and ΔG) were calculated and it was observed that increases on the adsorption temperature lead to increases on the amount adsorbed, indicating that the adsorption of PR-3B on C-PW and AC-PW followed endothermic processes.

For treatment of simulated industrial textile effluents, the AC-PW adsorbent presented very good performance for removing at least 98% of the mixture of dyes in a medium containing high saline concentrations.

Notations

a_{RP}	the Redlich-Peterson constants $(mg\,L^{-1})^{-g}$
C	constant related with the thickness of boundary layer $(mg\,g^{-1})$

C_f dye concentration at ending of the adsorption ($mg\,L^{-1}$)
C_e dye concentration at the equilibrium ($mg\,L^{-1}$)
C_o initial dye concentration put in contact with the adsorbent ($mg\,L^{-1}$)
g dimensionless exponent of Redlich-Peterson equation
h_o the initial sorption rate ($mg\,g^{-1}\,h^{-1}$) of pseudo-second order equation
k_{AV} is the Avrami kinetic constant (h^{-1})
k_f the pseudo-first-order rate constant (h^{-1})
K_F the Freundlich equilibrium constant ($mg\,g^{-1}(mg\,L^{-1})^{-1/n_F}$)
k_{id} the intra-particle diffusion rate constant ($mg\,g^{-1}\,h^{-0.5}$)
K_L the Langmuir equilibrium constant ($L\,mg^{-1}$)
K_{RP} the Redlich-Peterson equilibrium constant ($L\,g^{-1}$)
K_S the Sips equilibrium constant ($(mg\,L^{-1})^{-1/n_s}$)
k_s the pseudo-second order rate constant ($g\,mg^{-1}\,h^{-1}$)
m mass of adsorbent (g)
n_{AV} is a fractionary reaction order (Avrami) which can be related, to the adsorption mechanism
n_F dimensionless exponent of the Freundlich equation
n_S dimensionless exponent of the Sips equation
q amount adsorbed of the dye by the adsorbent ($mg\,g^{-1}$)
q_e amount adsorbate adsorbed at the equilibrium ($mg\,g^{-1}$)
Q_{max} the maximum adsorption capacity of the adsorbent ($mg\,g^{-1}$)
q_t amount of adsorbate adsorbed at time ($mg\,g^{-1}$)
t time of contact (h)
V volume of dye solution put in contact with the adsorbent (L)

Greek letters
α the initial adsorption rate ($mg\,g^{-1}\,h^{-1}$) of the Elovich Equation
β Elovich constant related to the extent of surface coverage and also to the activation energy involved in chemisorption ($g\,mg^{-1}$)

Acknowledgements

The authors are grateful to Ministério de Ciência e Tecnologia (MCT), and to Conselho Nacional de Desenvolvimento Científico e Tecnológico (CNPq) for financial support and fellowships. We also thank to Dr. Ryan Coleman White for language improvements.

References

[1] E.C. Lima, B. Royer, J.C.P. Vaghetti, N.M. Simon, B.M. da Cunha, F.A. Pavan, E.V. Benvenutti, R.C. Veses, C. Airoldi, Application of Brazilian-pine fruit coat as a biosorbent to removal of reactive red 194 textile dye from aqueous solution. Kinetics and equilibrium study, J. Hazard. Mater. 155 (2008) 536–550.
[2] F.A. Pavan, Y. Gushikem, A.S. Mazzocato, S.L.P. Dias, E.C. Lima, Statistical design of experiments as a tool for optimizing the batch conditions to methylene blue biosorption on yellow passion fruit and mandarin peels, Dyes Pigments 72 (2007) 256–266.
[3] R.O.A. de Lima, A.P. Bazo, D.M.F. Salvadori, C.M. Rech, D.P. Oliveira, G.A. Umbuzeiro, Mutagenic and carcinogenic potential of a textile azo dye processing plant effluent that impacts a drinking water source, Mutat. Res. 626 (2007) 53–60.
[4] F.A. Pavan, S.L.P. Dias, E.C. Lima, E.V. Benvenutti, Removal of congo red from aqueous solution by anilinepropylsilica xerogel, Dyes Pigments 76 (2008) 64–69.
[5] V.K. Gupta, I.A. Suhas, D. Mohan, Equilibrium uptake and sorption dynamics for the removal of a basic dye (basic red) using low-cost adsorbents, J. Colloid Interface Sci. 265 (2003) 257–264.
[6] V.K. Gupta, D. Mohan, V.K. Saini, Studies on the interaction of some azo dyes (naphthol red-J and direct orange) with nontronite mineral, J. Colloid Interface Sci. 298 (2006) 79–86.
[7] S. Wang, H.T. Li, Kinetic modelling and mechanism of dye adsorption on unburned carbon, Dyes Pigments 72 (2007) 308–314.
[8] F.A. Pavan, E.C. Lima, S.L.P. Dias, A.C. Mazzocato, Methylene blue biosorption from aqueous solutions by yellow passion fruit waste, J. Hazard. Mater. 150 (2008) 703–712.
[9] B. Royer, N.F. Cardoso, E.C. Lima, V.S.O. Ruiz, T.R. Macedo, C. Airoldi, Organofunctionalized kenyaite for dye removal from aqueous solution, J. Colloid Interface Sci. 336 (2009) 398–405.
[10] D. Kavitha, C. Namasivayam, Capacity of activated carbon in the removal of acid brilliant blue: Determination of equilibrium and kinetic model parameters, Chem. Eng. J. 139 (2008) 453–461.
[11] H. Marsh, F.R. Reinoso, Activated Carbon, Elsevier, Amsterdam, 2006, p. 554.
[12] A.N.A. El-Hendawy, An insight into the KOH activation mechanism through the production of microporous activated carbon for the removal of Pb^{2+} cations, Appl. Surf. Sci. 255 (2009) 3723–3730.
[13] W. Li, K. Yang, J. Peng, L. Zhang, S. Guo, H. Xia, Effects of carbonization temperatures on characteristics of porosity in coconut shell chars and activated carbons derived from carbonized coconut shell chars, Ind. Crops Prod. 28 (2008) 190–198.
[14] A.S. Albero, J.S. Albero, A.S. Escribano, F.R. Reinoso, Ethanol removal using activated carbon: effect of porous structure and surface chemistry, Micropor. Mesopor. Mater. 120 (2009) 62–68.
[15] J.M. Dias, M.C.M. Alvim-Ferraz, M.F. Almeida, J. Rivera-Utrilla, M. Sánchez-Polo, Waste materials for activated carbon preparation and its use in aqueous-phase treatment: a review, J. Environ. Manage. 85 (2007) 833–846.
[16] M.P. Elizalde-González, J. Mattusch, A.A. Peláez-Cid, R. Wennrich R., Characterization of adsorbent materials prepared from avocado kernel seeds: natural, activated and carbonized forms, J. Anal. Appl. Pyrolysis 78 (2007) 185–193.
[17] B. Royer, N.F. Cardoso, E.C. Lima, J.C.P. Vaghetti, N.M. Simon, T. Calvete, R.C. Veses, Applications of Brazilian-pine fruit shell in natural and carbonized forms as adsorbents to removal of methylene blue from aqueous solutions—kinetic and equilibrium study, J. Hazard. Mater. 164 (2009) 1213–1222.
[18] J.L. Brasil, R.R. Ev, C.D. Milcharek, L.C. Martins, F.A. Pavan, A.A. dos Santos-Jr, S.L.P. Dias, J. Dupont, C.P.Z. Noreña, E.C. Lima, Statistical design of experiments as a tool for optimizing the batch conditions to Cr(VI) biosorption on *Araucaria angustifolia* wastes, J. Hazard. Mater 133 (2006) 143–153.
[19] E.C. Lima, B. Royer, J.C.P. Vaghetti, J.L. Brasil, N.M. Simon, A.A. dos Santos-Jr., F.A. Pavan, S.L.P. Dias, E.V. Benvenutti, E.A. da Silva, Adsorption of Cu(II) on *Araucaria angustifolia* wastes: determination of the optimal conditions by statistic design of experiments, J. Hazard. Mater. 140 (2007) 211–220.
[20] L.T. Arenas, J.C.P. Vaghetti, C.C. Moro, E.C. Lima, E.V. Benvenutti, T.M.H. Costa, Dabco/silica sol–gel hybrid material. The influence of the morphology on the $CdCl_2$ adsorption capacity, Mater. Lett. 58 (2004) 895–898.
[21] R.A. Jacques, R. Bernardi, M. Caovila, E.C. Lima, F.A. Pavan, J.C.P. Vaghetti, C. Airoldi, Removal of Cu(II), Fe(III) and Cr(III) from aqueous solution by aniline grafted silica gel, Sep. Sci. Technol. 42 (2007) 591–609.
[22] L.T. Arenas, E.C. Lima, A.A. dos, J.C.P. Santos-Junior, T.M.H. Vaghetti, E.V. Costa, Benvenutti, Use of statistical design of experiments to evaluate the sorption capacity of 1,4-diazoniabicycle[2,2,2]octane/silica chloride for Cr(VI) adsorption, Colloids Surf. A 297 (2007) 240–248.
[23] A.E. Ofomaja, Y.S. Ho, Effect of pH on cadmium biosorption by coconut copra meal, J. Hazard. Mater. 139 (2007) 356–362.
[24] E.C. Lima, F.J. Krug, M.A.Z. Arruda, Direct determination of lead in sweet fruit-flavored powder drinks by electrothermal atomic absorption spectrometry, Spectrochim. Acta B 53 (1998) 601–611.
[25] J.C.P. Vaghetti, E.C. Lima, B. Royer, B.M. da Cunha, N.F. Cardoso, J.L. Brasil, S.L.P. Dias, Pecan nutshell as biosorbent to remove Cu(II), Mn(II) and Pb(II) from aqueous solutions, J. Hazard. Mater. 162 (2009) 270–280.
[26] J.C.P. Vaghetti, E.C. Lima, B. Royer, J.L. Brasil, B.M. da Cunha, N.M. Simon, N.F. Cardoso, C.P.Z. Noreña, Application of Brazilian-pine fruit coat as a biosorbent to removal of Cr(VI) from aqueous solution. Kinetics and equilibrium study, Biochem. Eng. J. 42 (2008) 67–76.
[27] J.C.P. Vaghetti, E.C. Lima, B. Royer, N.F. Cardoso, B. Martins, T. Calvete, Pecan nutshell as biosorbent to remove toxic metals from aqueous solution, Sep. Sci. Technol. 44 (2009) 615–644.
[28] E.C.N. Lopes, F.S.C. dos Anjos, E.F.S. Vieira, A.R. Cestari, An alternative Avrami equation to evaluate kinetic parameters of the interaction of Hg(II) with thin chitosan membranes, J. Colloid Interface Sci. 263 (2003) 542–547.
[29] A.R. Cestari, E.F.S. Vieira, J.D.S. Matos, D.S.C. dos Anjos, Determination of kinetic parameters of Cu(II) interaction with chemically modified thin chitosan membranes, J. Colloid Interface Sci. 285 (2005) 288–295.
[30] A.R. Cestari, E.F.S. Vieira, A.A. Pinto, E.C.N. Lopes, Multistep adsorption of anionic dyes on silica/chitosan hybrid 1. Comparative kinetic data from liquid- and solid-phase models, J. Colloid Interface Sci. 292 (2005) 363–372.
[31] A.R. Cestari, E.F.S. Vieira, G.S. Vieira, L.E. Almeida, The removal of anionic dyes from aqueous solutions in the presence of anionic surfactant using aminopropylsilica—a kinetic study, J. Hazard. Mater. 138 (2006) 133–141.
[32] E.F.S. Vieira, A.R. Cestari, E.C.N. Lopes, L.S. Barreto, G.S. Lázaro, L.E. Almeida, Determination of kinetic parameters from isothermal calorimetry for interaction processes of pyrimethamine with chitosan derivatives, React. Funct. Polym. 67 (2007) 820–827.
[33] C.E. Zubieta, P.V. Messina, C. Luengo, M. Dennehy, O. Pieroni, P.C. Schulz, Reactive dyes remotion by porous TiO_2-chitosan materials, J. Hazard. Mater. 152 (2008) 765–777.
[34] P. Leechart, W. Nakbanpote, P. Thiravetyan, Application of 'waste' wood-shaving bottom ash for adsorption of azo reactive dye, J. Environ. Manage. 90 (2009) 912–920.
[35] D.D. Asouhidou, K.S. Triantafyllidis, N.K. Lazaridis, K.A. Matis, S.S. Kim, T.J. Pinnavaia, Sorption of reactive dyes from aqueous solutions by ordered hexagonal and disordered mesoporous carbons, Micropor. Mesopor. Mater. 117 (2009) 257–267.